Chapter 5

Ratcheting Fatigue Behaviour of the Alloys at Elevated Temperatures

5.1 INTRODUCTION

This chapter discusses ratcheting fatigue behaviour of the modified 9Cr -1Mo steel and Inconel 617 alloy at their respective service temperatures of 600^{o}C and 750-850^{o}C, under the effect of mean stress. Ratcheting is basically due to non-zero mean stress; thus, for both the alloys ratcheting studies have been performed under the influence of mean stress. Service temperature of the Inconel 617 alloy varies from 750-850^{o}C; therefore, an average temperature of 800^{o}C has been considered for the study. A similar study, on the effect of service temperature on ratcheting fatigue, has recently been conducted on Zircaloy-2, at 400^{o}C, by Rajpurohit et al., (2018). It was found that with increase in the mean stress, ratcheting strain increased and fatigue life was decreased. Rajpurohit et al., (2020) also reported comparative evaluation of ratcheting fatigue of Zircaloy-2 with respect to temperature at RT, 300^{o}C and 400^{o}C. It was observed that with rise in temperature, there was enhancement in fatigue life of the material and this was due to DSA in the temperature range of 300^{o}C to 400^{o}C. Kang et al., (2011) conducted a comparative study of ratcheting behaviour of metals with different crystal structures. It was concluded that ratcheting behaviour not only depends upon the crystal structure or the fault energy, but also influenced by the variation in mobility of dislocations.This chapter, apart from comparison of ratcheting fatigue behaviour of both the materials (modified 9Cr -1Mo steel and Inconel 617 alloy) at their service temperatures, also presents comparison of their ratcheting fatigue behaviour at the homologous temperature of 0.42 T_m, along with their fractographic studies and deformation behaviour. Fractographic analysis of the failed specimens was performed with the aid of SEM. Microstructural characterization along with the study of dislocation substructure was carried out by TEM.

5.2 Ratcheting fatigue behaviour of modified 9Cr-1Mo steel at 600°C

5.2.1 Tensile properties of modified 9Cr-1Mo steel at 600°C

Tensile tests were conducted at strain rate of 10^{-3} s^{-1} to assess various tensile properties at 600°C and to decide matrix for ratcheting fatigue experiments. All tests were performed above the yield strength of the alloy. The tensile properties of the modified 9Cr-1Mo steel tested at the strain rate of 10^{-3} s^{-1} at RT and 600°C is given in Table 5.1.

Table 5.1 Tensile properties of the modified 9Cr-1Mo steel tested at the strain rate of 10^{-3} s^{-1}, at RT and 600°C.

Temperature (°C)	Yield Strength (MPa)	Ultimate Tensile Strength (MPa)	Elongation (%)	Uniform plastic elongation (%)	Reduction in area (%)	Elastic modulus (GPa)
RT	580	712	25.8	9.2	74	210
600°C	310	380	34.7	1.8	92	150

5.2.2 Uniaxial ratcheting fatigue behaviour of modified 9Cr-1Mo steel at 600°C under the effect of mean stress

For understanding the influence of tensile mean stress on the accumulation of ratcheting strain and fatigue life, fatigue tests were carried out with asymmetric stress cycling at different mean stress, varying maximum stress and minimum stress, keeping the stress amplitudeand stress rate constant at 270 MPa and 150 MPa/s respectively. Ratcheting cyclic life is presented in Table 5.2 for the mean stress varying in the range from 45 to 95 MPa. It may be seen from Table 5.2 that the number of cycles to failure (N_f) decreased with rise in the mean stress from 45 to 95 MPa.

Table 5.2 Dependence of cyclic life of modified 9Cr-1Mo, under asymmetric loading steel at varying mean stress, at constant stress amplitude of 270 MPa and stress rate of 150 MPa/s at 600^{o}C.

S.No.	Maximum stress (σ_{max}) MPa	Minimum stress (σ_{min}) MPa	Mean stress (σ_m) MPa	No. of cycles to failure (N_f)
1	315	-225	**45**	5003
2	340	-200	**70**	4157
3	365	-175	**95**	2894

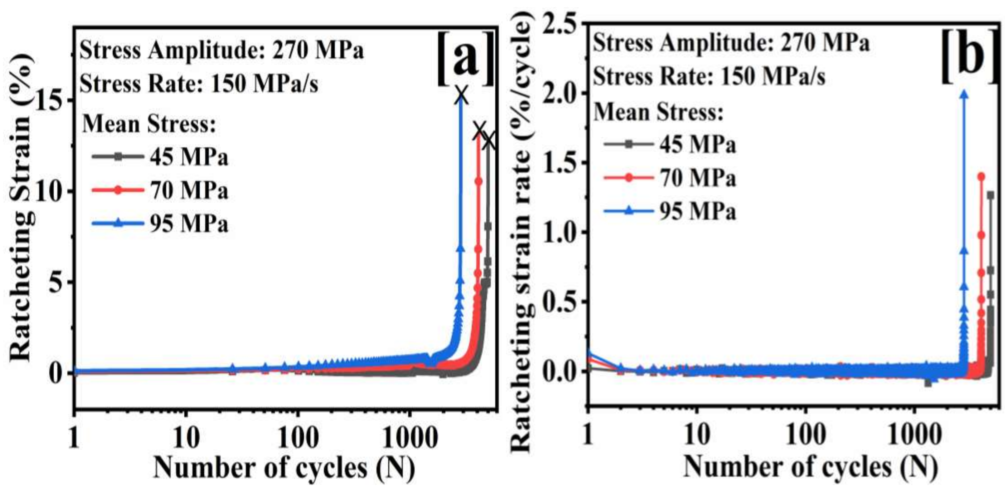

Fig. 5.1 Influence of mean stress on ratcheting behaviour of modified 9Cr-1Mo steel, at 600^{o}C showing: (a) variation of ratcheting strain with cycles under different mean stress and (b) variation of ratcheting strain rate with cycles.

Fig. 5.1(a) depicts the change in the accumulating ratcheting strain and Fig. 5.1(b) shows rate of accumulation of ratcheting strain with cycles to failure, at varying mean stresses. The results show high rate of accumulation of plastic strain with rise in mean stress from 45 to 95 MPa. Similarly, accumulation of ratcheting strain also increased from a rise in the mean stress, thereby fatigue life was reduced.

5.2.3 Fracture behaviour of modified 9Cr-1Mo steel at 600^{o}C

Fracture behaviour of all the samples tested at 600^{o}C, under different mean stresses was characterized by SEM. Since the loading was asymmetric and a tensile mean stress was acting on the specimen continuously, the specimens failed in ductile manner exhibiting cup and cone type fracture.

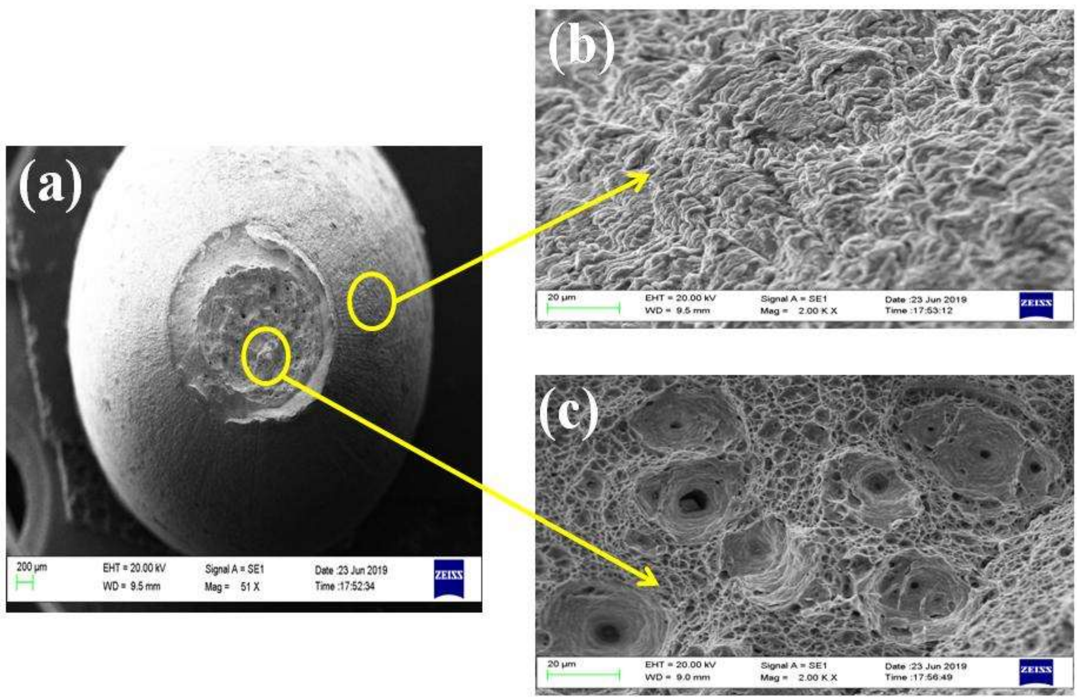

Fig. 5.2 Fracture surface of modified 9 Cr-1Mo steel ratcheted at 600^{o}C: (a) full view of the fracture surface (b) magnified view of the annular region, below the fracture surface, showing striations like features and (c) magnified view of the central region of the fracture surface showing dimples.

Examination of the specimens fractured from ratcheting fatigue revealed two distinct regions one of light contrast and annular shape, and the other of darker contrast and flat shape. While the annular region shows tapering, the central region is flat (Fig.5.2a) as already observed in case of modified 9Cr-1Mo at room temperature. The examination of the annular region at higher magnification revealed distinct features like fatigue striations (Fig. 5.2b) whereas the central flat region shows dimples (Fig. 5.2 c).

5.2.4 Comparison of uniaxial ratcheting behaviour of modified 9Cr-1Mo steel at 600°C and RT.

For comparing the ratcheting fatigue behaviour of modified 9Cr-1Mo steel at the service temperature of 600°C with that at RT, mean stress and stress amplitude are normalized with respect to ultimate tensile strength of the alloy at the test temperatures to have indentical ratios at constant stress rate. Table 5.3 depicts the test matrix for modified 9Cr-1Mo steel at RT and 600 °C at constant normalized mean stress of 0.18, normalized stress amplitude of 0.71 and stress rate of 150 MPa/s.

Table 5.3 Ratcheting fatigue test matrix of modified 9Cr-1Mo steel at RT and 600 °C, at constant normalized mean stress of 0.18, normalized stress amplitude of 0.71 and stress rate of 150 MPa/s.

Temperature (°C)	Maximum stress σ_{max} (MPa)	Minimum stress σ_{min} (MPa)	Stress Amplitude σ_a (MPa)	Mean stress σ_m (MPa)	Normalized stress amplitude (σ_a / σ_{UTS})	Normalized mean stress (σ_m / σ_{UTS})	No. of cycles to failure (N_f)
RT	634	-378	131	506	128/713 = 0.18	506/713 =0.71	330
600 °C	340	-200	70	270	70/380 = 0.18	270/380 = 0.71	4157

Cyclic life is higher at service temperature of 600 °C in comparison to that at RT. Fig. 5.3 shows that that ratcheting strain (Fig. 5.3a) and ratcheting strain rate (Fig. 5.3b) decreases with increase in temperature.

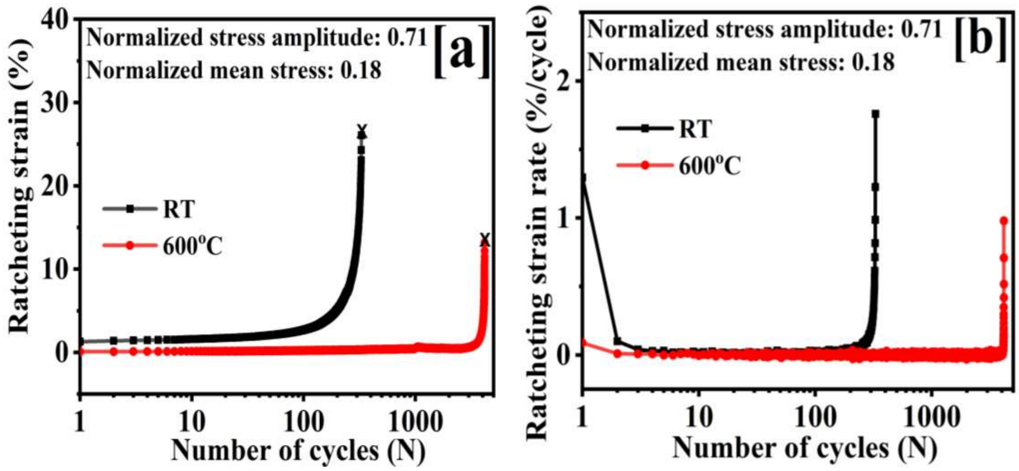

Fig. 5.3 Influence of temperature on ratcheting behaviour of modified 9Cr-1Mo steel: (a) variation of ratcheting strain with cycles and (b) variation of ratcheting strain rate with cycles atconstant normalized mean stress of 0.18, normalized stress amplitude of 0.71 and stress rate of 150 MPa/s at RT and 600 °C.

5.3 Ratcheting fatigue behaviour of Inconel 617 alloy at 800°C

5.3.1 Tensile properties of Inconel 617 alloy at 800°C

Tensile tests were conducted at strain rate of 10^{-3} s^{-1} to assess various tensile properties at 800°C and to decide matrix for ratcheting fatigue tests. All tests were performed above the yield strength of the alloy. The tensile properties of the Inconel 617 alloy tested at the strain rate of 10^{-3} s^{-1} at RT and 800°C are given in Table 5.4.

Table 5.4 Tensile properties of the Inconel 617 alloy at the strain rate of 10^{-3} s^{-1}, at RT and 800°C.

Temperature (°C)	Yield Strength (MPa)	Ultimate Tensile Strength (MPa)	Elongation (%)	Uniform plastic elongation (%)	Reduction in area (%)	Elastic modulus (GPa)
RT	347	835	66	54	68	210
800°C	250	365	70	10	72	160

5.3.2 Uniaxial ratcheting fatigue behaviour of Inconel 617 alloy at 800°C under the effect of mean stress

Asymmetric load controlled cyclic tests were conducted for studying the influence of positive mean stress on ratcheting strain and cyclic life. The test matrix with maximum and minimum stress was designed in such a way that there is variation in the mean stress from 20 to 95 MPa, while keeping the stress amplitude and stress rate constant, at 255 MPa and 150 MPa/s respectively, (Table 5.5). It may also be observed that as the mean stress increases from 20 to 95 MPa, cyclic life decreases from 9409 to 110 cycles.

Table 5.5 Dependence of cyclic life of Inconel 617 alloy, under asymmetric loading at varying mean stress, tested at constant stress amplitude of 255 MPa and stress rate of 150 MPa/s at 800°C.

S.No.	Maximum stress (σ_{max}) MPa	Minimum stress (σ_{min}) MPa	Mean stress (σ_m) MPa	No. of cycles to failure (N_f)
1	275	-235	**20**	9409
2	300	-210	**45**	5774
3	325	-185	**70**	1735
4	350	-160	**95**	110

Fig. 5.4(a) shows the change in the ratcheting strain accumulation with cycles, up to failure (N_f), at varying mean stresses. The ratcheting strain accumulation for the first cycle increases from 5.35% to 9.90%, with increase in the mean stress from 20 to 95 MPa and fatigue life is decreased. The rate of accumulation of ratcheting strain was highest in the beginning and decreased up to about 20 cycles, there after remained nearly constant (Fig. 5.4b).

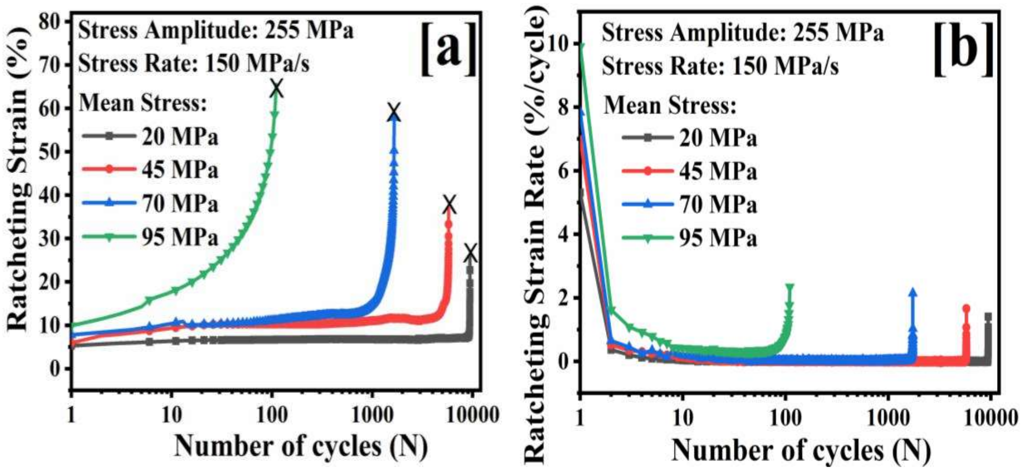

Fig. 5.4 Influence of mean stress on ratcheting behaviour of Inconel 617 alloy at 800^{o}C showing: (a) variation of ratcheting strain with cycles under different mean stresses (b) variation of ratcheting strain rate with cycles.

5.3.3 Fracture behaviour of Inconel 617 alloy at 800^{o}C

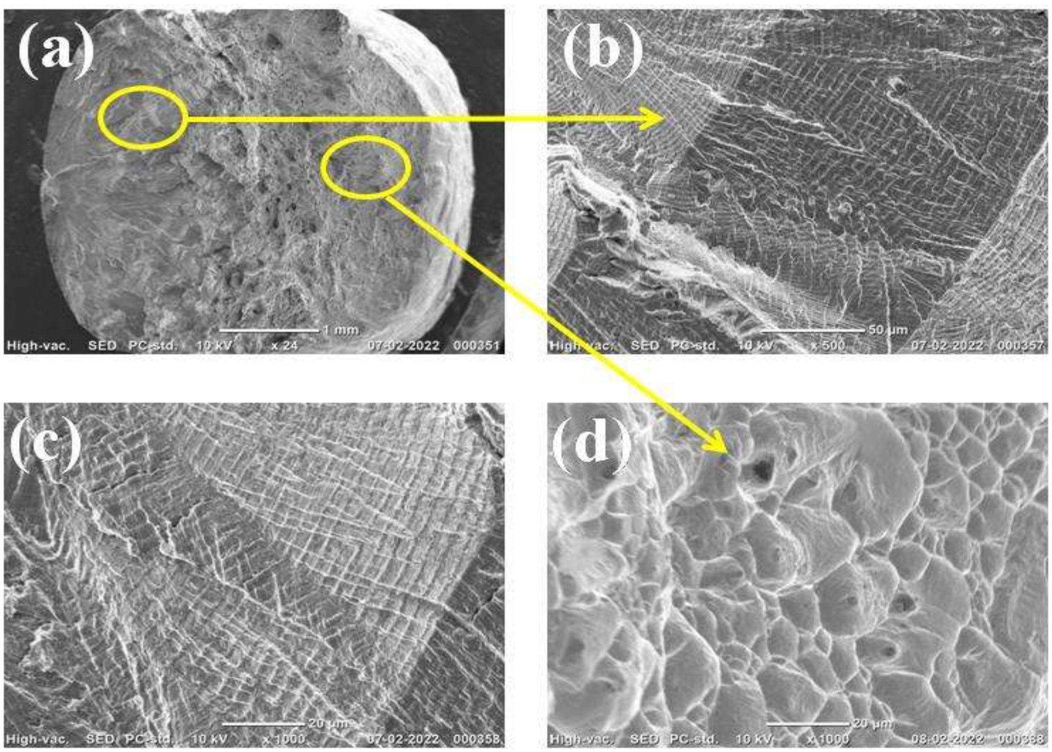

Fig. 5.5 Fracture surface of Inconel 617 alloy ratcheted at 800^{o}C: (a) full view of the fracture surface (b) magnified view of the fatigue region showing striations (c) magnified view of striations and (d) magnified view of the tensile region showing dimples.

Fracture behaviour of all the samples tested at 800°C, with mean stress, was characterized by SEM. Inconel 617 alloy exhibited characteristic fatigue fracture under asymmetrical cyclic loading, unlike the modified 9Cr-1Mo steel at its service temperature. The low magnification image depicts flat fracture surface (Fig. 5.5a), comprising of the regions of fatigue signature (Fig. 5.5b), and tensile overload (Fig. 5.5d). The magnified image from the region of fatigue fracture exhibited striations, signifying fatigue fracture (Fig. 5.5c). The vein like features in Fig. 5.5(c) are due to level difference.

5.3.4 Comparison of uniaxial ratcheting behaviour of Inconel 617 alloy at 800°C and RT.

For comparing the ratcheting fatigue behaviour of Inconel 617 alloy at respective service temperature of 800°C with that at RT, the mean stress and stress amplitude are normalized with respect to ultimate tensile strength of the alloys at that particular temperature at constant stress rate. Table 5.6 depicts the test matrix for Inconel 617 alloy at RT and 800°C at constant normalized mean stress of 0.69, normalized stress amplitude of 0.12 and stress rate of 150 MPa/s.

Table 5.6 Ratcheting fatigue test matrix of Inconel 617 alloy at RT and 800°C, at constant normalized mean stress of 0.69, normalized stress amplitude of 0.12 and stress rate of 150 MPa/s.

Temperature (°C)	Maximum stress σ_{max} (MPa)	Minimum stress σ_{min} (MPa)	Stress Amplitude σ_a (MPa)	Mean stress σ_m (MPa)	Normalized stress amplitude (σ_a / σ_{UTS})	Normalized mean stress (σ_m / σ_{UTS})	No. of cycles to failure (N_f)
RT	676	-476	576	100	576/835 = 0.69	100/835 = 0.12	634
800°C	300	-210	255	45	255/365 = 0.69	45/365 = 0.12	5774

Cyclic life is higher at service temperature of 800°C in comparison with that at RT. Fig. 5.6 shows that ratcheting strain (Fig. 5.6a) and ratcheting strain rate (Fig. 5.6b) decreases with increase in temperature, thus there is enhancement of fatigue life of the alloy with rise in temperature.

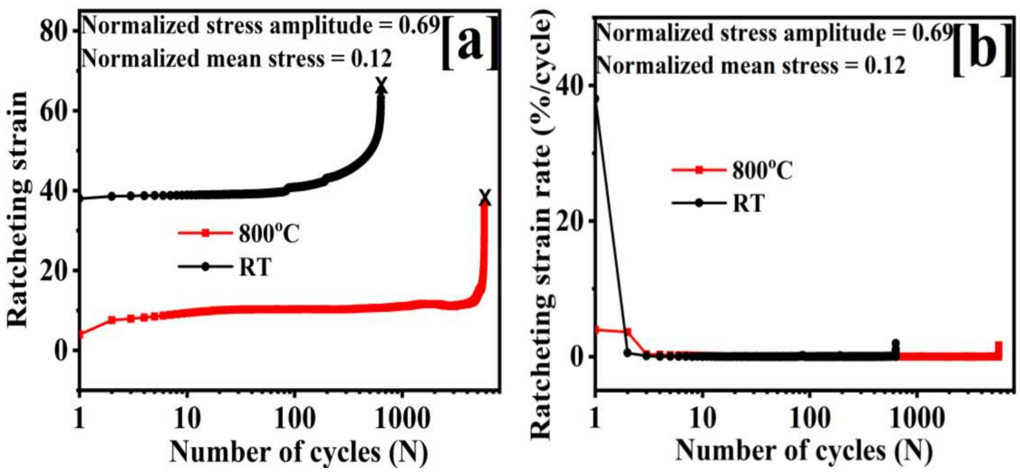

Fig. 5.6 Influence of temperature on ratcheting behaviour of Inconel 617 alloy: (a) variation of ratcheting strain with cycles and (b) variation of ratcheting strain rate with cycles at constant normalized mean stress of 0.69, normalized stress amplitude of 0.12 and stress rate of 150 MPa/s at RT and 800°C.

5.4 Comparison of both the alloys at homologous temperature

5.4.1 Homologous temperature and its calculation

The best way to compare the mechanical properties of different materials at elevated temperatures is in terms of the ratio of the test temperature to the melting point, expressed in degrees Kelvin. This ratio is often referred to as the homologous temperature.

Mathematically homologous temperature is expressed as**:**

$$T_H = \frac{T}{T_m} \tag{5.1}$$

where; T_H: homologous temperature

T: service temperature in Kelvin

T_m: melting temperature in Kelvin

Since the service temperature of modified 9Cr-1Mo steel is lower than that of Inconel 617 alloy; therefore for calculation of homologous temperature the service temperature of modified 9Cr-1Mo steel (873 K) has been taken into consideration.

Melting point of modified 9Cr-1Mo steel: 2073 K

Melting point of Inconel 617 alloy: 1623 K

Service temperature of modified 9Cr-1Mo steel: 873 K

Service temperature of Inconel 617 alloy: 1123 K [Dekhane., 2013;Special metals].

Thus, for modified 9Cr-1Mo steel:

$$\boldsymbol{T_H = \frac{873}{2073}}$$

$$\boldsymbol{T_H = 0.42}$$

Hence, for comparison the homologous temperature is kept identical and the corresponding temperature for Inconel 617 alloy is calculated as:

$$\boldsymbol{T_H = \frac{T}{T_m}}$$

$$\boldsymbol{0.42 = \frac{T}{1623}}$$

$$\boldsymbol{T = 682K}$$

The service temperature of modified 9Cr-1Mo steel is 600^{o}C, thus using the same homologous temperature of 0.42, the corresponding temperature for Inconel 617 alloy works out to be 409^{o}C.

5.4.2 Tensile properties of both the alloys at 0.42 T_m

Tensile tests were conducted at strain rate of 10^{-3} s $^{-1}$ to assess various tensile parameters and to prepare matrix for ratcheting fatigue experiments. All the tests were performed above the yield strength of materials. The tensile properties of the alloys tested at the strain rate of 10^{-3} s^{-1} are given in Table 5.7

Table 5.7 Tensile properties of the alloys tested at strain rate of 10^{-3} s^{-1}, at 0.42 T_m.

Material	Yield Strength (MPa)	Ultimate Tensile Strength (MPa)	Elongation (%)	Uniform plastic elongation (%)	Reduction in area (%)	Degree of work hardening (S_{UTS} /S_{YS})
Modified 9Cr-1Mo steel	305	380	34.7	2.2	92	1.24
Inconel 617 alloy	235	665	72	60	63	2.82

5.4.3 Uniaxial ratcheting behaviour of the alloys at 0.42 T_m

Set of experiments were conducted at 0.42 T_m to confirm and compare the behaviour of the two materials, with the help of normalized mean stress and stress amplitude, at constant stress rate of 150 MPa/s. Since there is difference in the yield strength and ultimate tensile strength of the two materials under study, the maximum stress will differ, due to which mean stress and stress amplitude will vary, hence comparison of the two materials will not be possible. Therefore, the mean stress and amplitude were normalized with respect to ultimate tensile strength, and the stress rate was kept constant. There is variation in service temperatures of the two alloys; hence, tests of the two alloys were conducted at the same homologous temperature of 0.42.

The test matrix at 0.42 $T_{m,}$ at constant normalized stress amplitude of 0.71, normalized mean stress of 0.12, and stress rate of 150 MPa/s is given in Table 5.8. It can be very well observed that under these parameters the fatigue life for modified 9Cr-1Mo steel is higher in comparison to Inconel 617 alloy.

Table 5.8 Ratcheting fatigue test matrix of the alloys, at 0.42 T_m at constant normalized stress amplitude of 0.71, normalized mean stress of 0.12 and stress rate of 150 MPa/s.

Material	Maximum stress σ_{max} (MPa)	Minimum stress σ_{min} (MPa)	Stress Amplitude σ_a (MPa)	Mean stress σ_m (MPa)	Normalized stress amplitude (σ_a / σ_{UTS})	Normalized mean stress (σ_m / σ_{UTS})	No. of cycles to failure (N_f)
Modified 9Cr-1Mo steel	315	-225	270	45	270/380 = 0.71	45/380 = 0.12	5003
Inconel 617 alloy	551	-395	473	78	473/665 = 0.71	78/665 = 0.12	3364

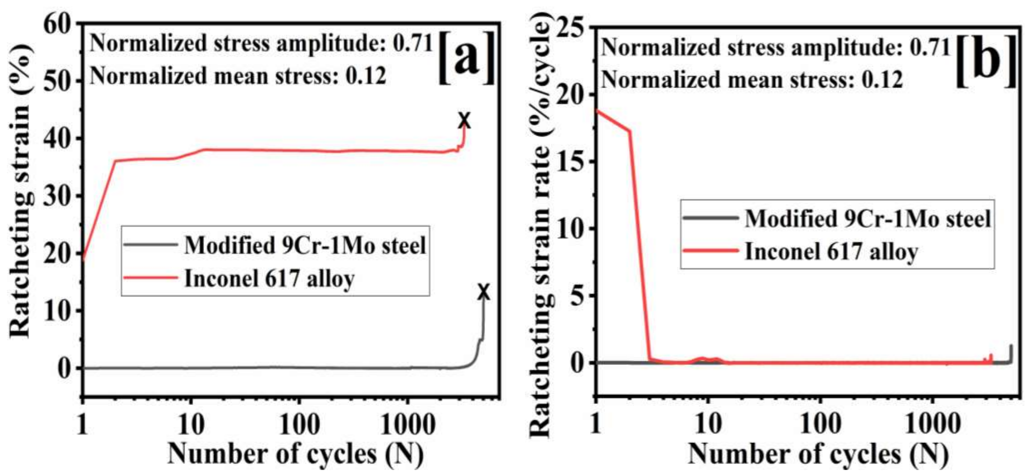

Fig. 5.7 (a) Variation of cumulative ratcheting strain accumulation and (b) variation of ratcheting strain rate with cycles for modified 9Cr-1Mo steel and Inconel 617 alloy at 0.42 T_m at constant normalized stress amplitude of 0.71, normalized mean stress of 0.12 and stress rate of 150 MPa/s.

Fig. 5.7(a and b) depicts the ratcheting strain and ratcheting strain rate plot for both the alloys under the above mentioned parameters. Ratcheting strain accumulation in Inconel 617 alloy is very high (20%) in comparison to modified 9Cr-1Mo steel. From the ratcheting strain plot it can be observed that during initial cycles the strain accumulation is very high and then it stabilizes and can be seen from the ratcheting strain rate plot that both the lines coincides (Fig. 5.7b).

One unique feature in the plot of the Inconel 617 alloy is that after the first cycle of asymmetrical stressing there is sudden increase in strain in the second cycle, beyond that it remains almost constant (Fig. 5.7a). The variation in ratcheting strain rate of the two alloys is depicted in Fig. 5.7(b).

Another set of experiment was conducted at 0.42 T_m at constant normalized stress amplitude of 0.71, normalized mean stress of 0.18 and stress rate of 150 MPa/s. Cyclic life in case of modified 9Cr-1Mo steel is higher in comparison to Inconel 617 alloy (Table 5.9). Ratcheting strain as well as its rate of accumulation is very high in Inconel 617 alloy (45%) as compared to modified 9Cr-1Mo steel (Fig. 5.8a and b). Abrupt stepped increase in ratcheting strain was observed before failure (Fig. 5.8a).

Table 5.9 Ratcheting fatigue test matrix of the alloys, at 0.42 T_m at constant normalized stress amplitude of 0.71, normalized mean stress of 0.18 and stress rate of 150 MPa/s.

Material	Maximum stress σ_{max} (MPa)	Minimum stress σ_{min} (MPa)	Stress Amplitude σ_a (MPa)	Mean stress σ_m (MPa)	Normalized stress amplitude (σ_a / σ_{UTS})	Normalized mean stress (σ_m / σ_{UTS})	No. of cycles to failure (N_f)
Modified 9Cr-1Mo steel	340	-200	270	70	270/380 = 0.71	70/380 = 0.18	4157
Inconel 617 alloy	590	-350	473	120	473/665 = 0.71	120/665 = 0.18	2679

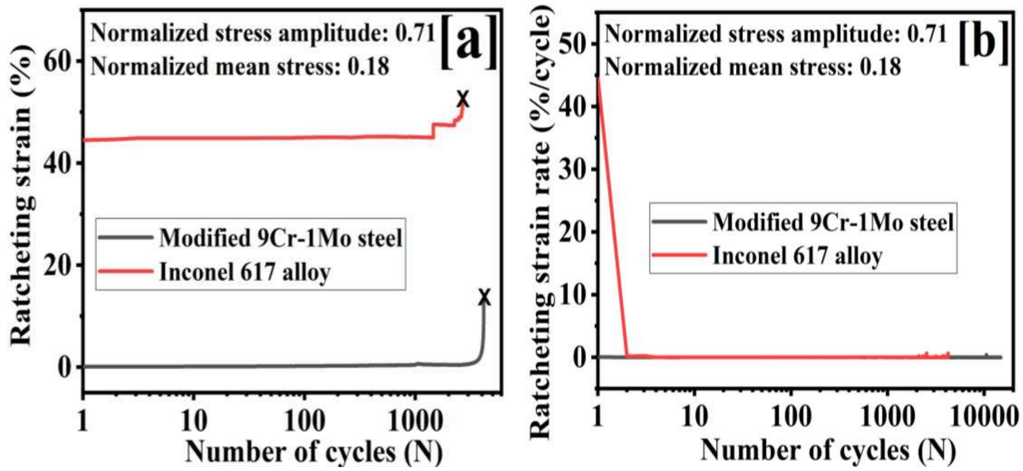

Fig. 5.8 (a) Variation of cumulative ratcheting strain accumulation and (b) variation of ratcheting strain rate with cycles for modified 9Cr-1Mo steel and Inconel 617 alloy at 0.42 T_m at constant normalized stress amplitude of 0.71, normalized mean stress of 0.18 and stress rate of 150 MPa/s.

For the confirmation as well as for comparison, one more set of experiment was conducted at 0.42 T_m at constant normalized stress amplitude of 0.71, normalized mean stress of 0.25 and stress rate of150 MPa/s. Similar results were observed as mentioned above. Cyclic life was higher for the modified 9Cr-1Mo steel in comparison with that of Inconel 617 alloy, as depicted in Table 5.10.

Table 5.10 Ratcheting fatigue test matrix of the alloys, at 0.42 T_m at constant normalized stress amplitude of 0.71, normalized mean stress of 0.25 and stress rate of 150 MPa/s.

Material	Maximum stress σ_{max} (MPa)	Minimum stress σ_{min} (MPa)	Stress Amplitude σ_a (MPa)	Mean stress σ_m (MPa)	Normalized stress amplitude (σ_a / σ_{UTS})	Normalized mean stress (σ_m / σ_{UTS})	No. of cycles to failure (N_f)
Modified 9Cr-1Mo steel	365	-175	270	95	270/380 = 0.71	95/380 = 0.25	2894
Inconel 617 alloy	640	-310	473	165	473/665 = 0.71	165/665 = 0.25	2252

Ratcheting strain and its rate of accumulation is very high in the Inconel 617 alloy (65%) as compared to that in the modified 9Cr-1Mo steel (Fig. 5.9a and b) and stepped increase in strain can be observed in Inconel 617 alloy from Fig. 5.9(a).

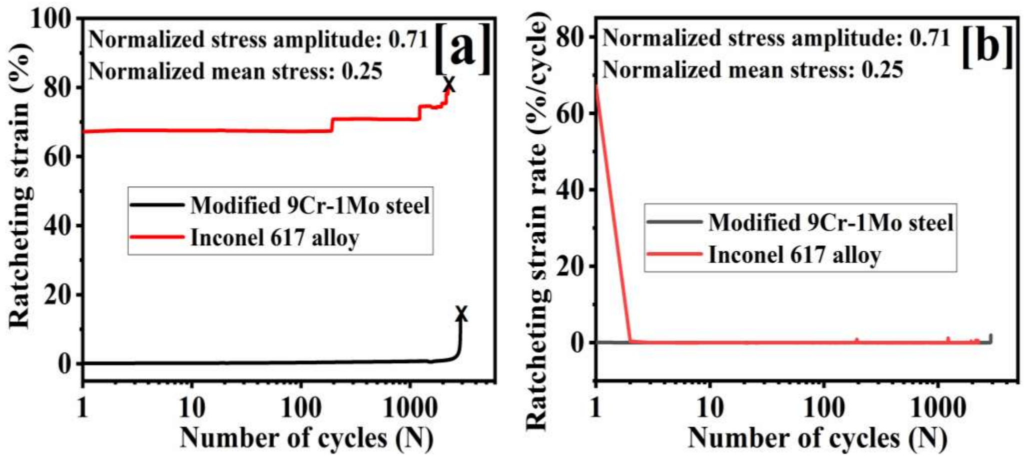

Fig. 5.9 (a) Variation of cumulative ratcheting strain accumulation and (b) variation of ratcheting strain rate with cycles for modified 9Cr-1Mo steel and Inconel 617 alloy at 0.42 T_m at constant normalized stress amplitude of 0.71, normalized mean stress of 0.25 and stress rate of 150 MPa/s.

5.4.4 Fracture behaviour of the alloys at 0.42 T_m

The ends of the fractured samples of both the alloys tested at 0.42 T_m were studied under scanning electron microscope. In case of modified 9Cr-1Mo steel Fig. 5.10(a) shows the full view of the fracture end exhibiting cup and cone type fracture. Fig. 5.10(b) shows the annular region, below the fracture surface, with striations like features. Fig.5.10(c) shows the fracture surface with dimples in central region. Inconel 617 alloy exhibits typical fatigue fracture (Fig. 5.11a). On magnifying the fatigue region shows striations at regular intervals (Fig. 5.11b) and the tensile region exhibits dimples (Fig. 5.11c).

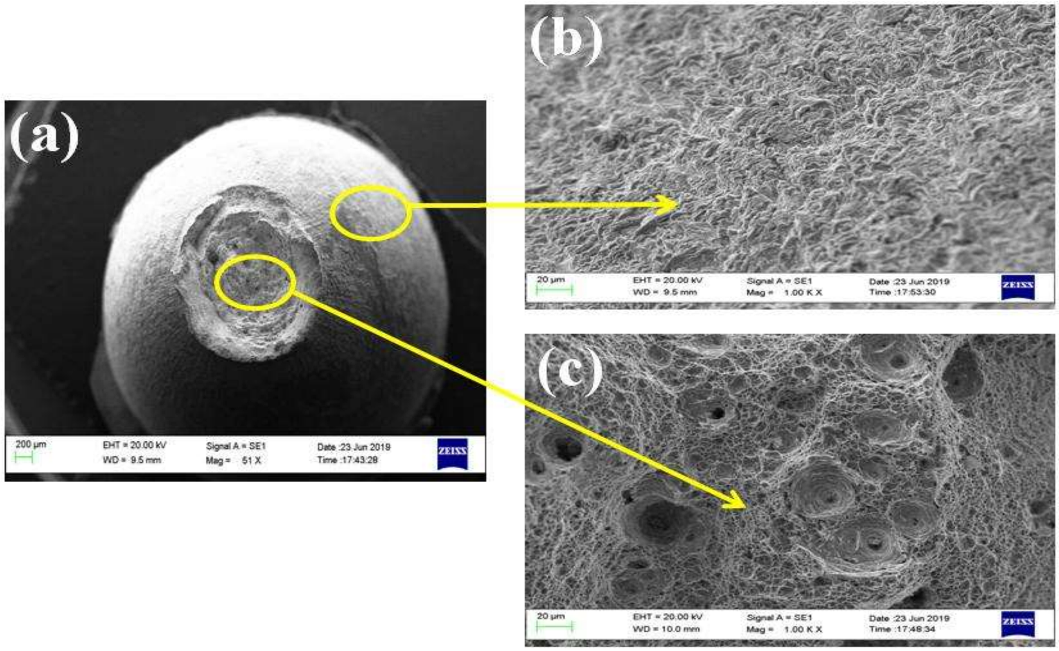

Fig. 5.10 Fracture surface of modified 9 Cr-1Mo steel ratcheted at 0.42 T_m: (a) full view of the fracture surface (b) magnified view of the annular surface, below fracture surface, showing striation like features and (c) magnified view of central region of the fracture surface showing dimples.

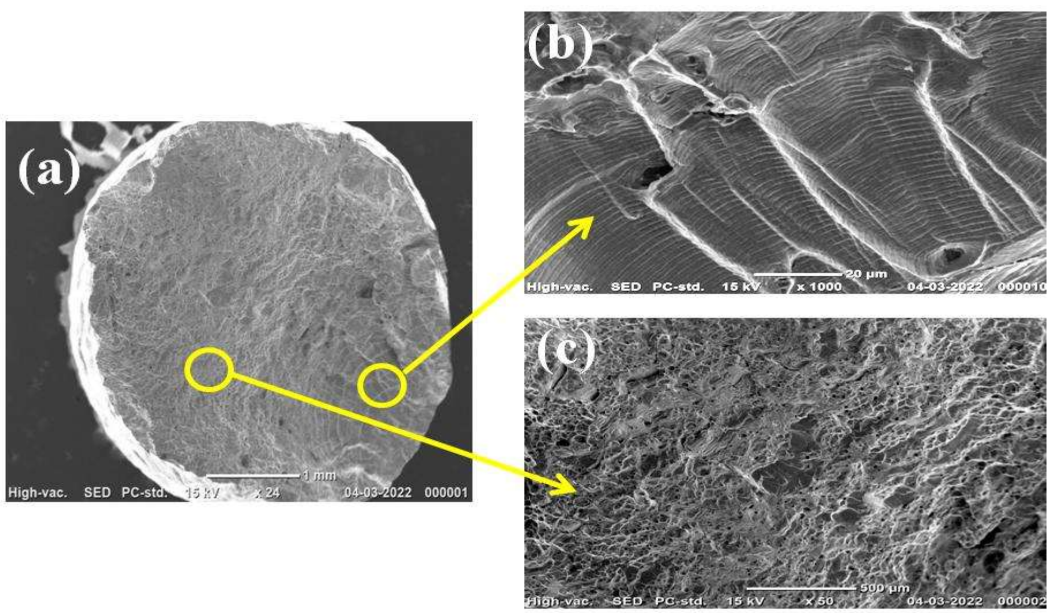

Fig. 5.11 Fracture surface of Inconel 617 alloy ratcheted at 0.42 T_m (a) full view of the fracture surface (b) magnified view of the fatigue region showing striations and (c) magnified view of the tensile region showing dimples.

5.5. DISCUSSION

5.5.1 Comparison of ratcheting fatigue behaviour of the alloys at RT and their respective service temperatures

On comparing the ratcheting behaviour at RT and service temperature for modified 9Cr-1Mo steel and Inconel 617 alloy it was observed that accumulation of ratcheting strain is higher at RT for both the alloys and there is reduction in cyclic life at RT as compared to that at the service temperatures. The deformation behaviour of modified 9Cr-1Mo steel at 600^{o}C under the effect of mean stress can be explained in terms of dislocation sub structure, precipitates, recovery and recrystallization.

At an elevated temperature of 600^{o}C at the lowest mean stress of 45 MPa dislocations are piled up at boundaries (Fig. 5.12a) and it is sufficient to initiate formation of dislocation cells that almost tend to form subgrains as depicted in Fig. 5.12(b). On further increase in the mean stress to 70MPa, fully recovered structure is observed to occur (Fig. 5.12c). At the highest mean stress of 95 MPa the onset of recrystallization was observed (Fig. 5.12d). In case of modified 9Cr-1Mo steel besides inducing recovery and recrystallization, the cyclic deformation in ratcheting mode also affected the chromium carbide precipitates, present along the lath boundaries prior to cyclic deformation as reported in Chapter 3.

The cyclic deformation can shear these precipitates, particularly the coherent ones, and cyclic loading for a larger number of cycles can even lead to their dissolution. The stage of dissolution could not be imaged in the present study as the specimens were ratcheted till fracture. It is known that large number of vacancies are produced during cyclic loading, these vacancies enhance the diffusion of elements, hence re-precipitation of the carbides (may be of a different chemical constitution or crystal structure) occurs within the recovered or recrystallized grains (marked by red arrows in Fig. 5.12d); the absence of the chromium carbides along the lath boundaries, can be a pointer to their prior dissolution.

The phenomenon of dynamic strain aging has been reported in the modified 9Cr-1Mo steel at 600°C under low cycle fatigue and observed to cause strengthening [Nagesha et al., 2002a; Nagesha et al., 2002b; Sarkar et al., 2012; Sarkar et al., 2013]. Thus, the strengthening of the specimens may be ascribed to reprecipitation of fine carbides and dynamic strain aging.

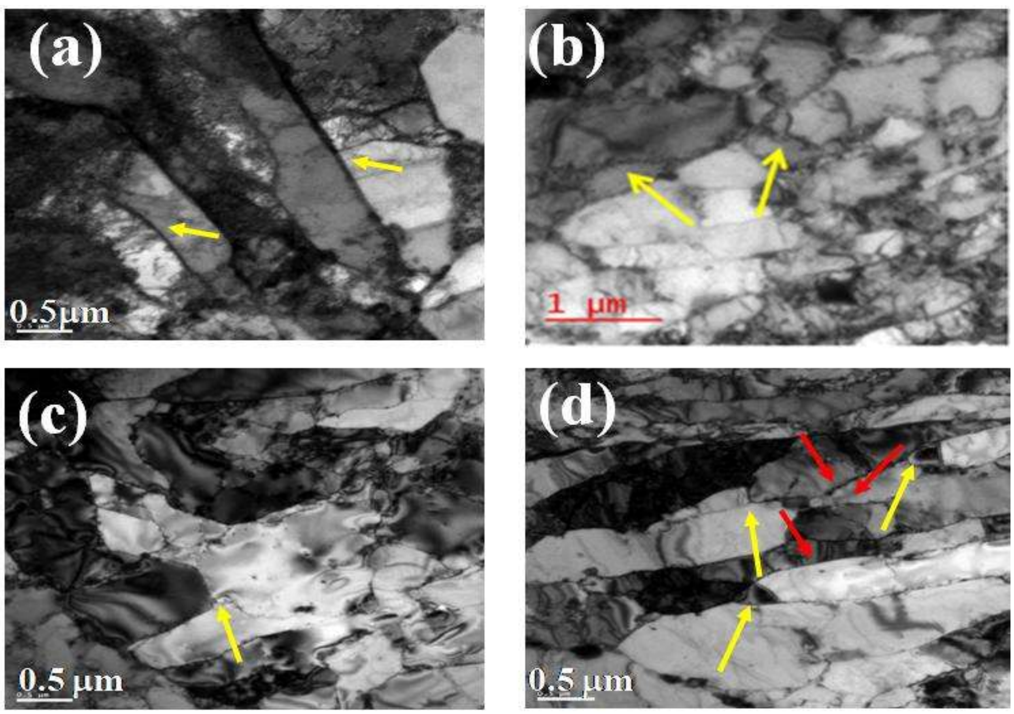

Fig. 5.12 Bright field TEM micrograph of the modified 9Cr-1Mo steel specimen tested at 600°C showing: (a) dislocation pile up at boundaries (b) dislocation cells (yellow arrows) in the specimen tested at mean stress of 45 MPa, stress amplitude of 270 MPa and stress rate of 150 MPa/s (c) complete recovery (yellow arrow) of specimen tested at mean stress of 80 MPa, stress amplitude of 235 MPa and stress rate of150 MPa/s and (d) beginning of recrystallization (yellow arrows) and re-precipitation of the carbides (red arrow) occurs within the recovered or recrystallized grains of the specimen tested at mean stress of 95 MPa, stress amplitude of 270 MPa and stress rate of 150 MPa/s.

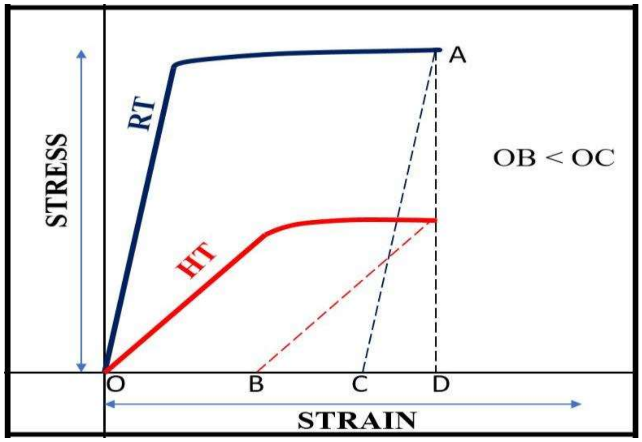

Fig. 5.13 Schematic tensile stress strain plot showing plastic strain at both the test temperatures.

There could also be the effect of lower modulus at 600°C and 800°C, on less accumulation of plastic strain, following unloading from the maximum stress. As shown below schematically in Fig 5.13, the modulus of elasticity at 600^{o}C [Zhao et al., 2017] and 800°C for the two alloys is lower than that at RT; therefore, the effective plastic strain at 600^{o}C and 800°C, on unloading from the maximum stress, above the yield stress and upto the UTS, will be relatively less than that at RT.

TEM micrographs of the samples fatigue tested at 800^{o}C under asymmetrical loading at mean stress of 45 MPa clearly indicate precipitation of carbides which are bigger in size and randomly distributed in the microstructure (Fig. 5.14a and c). There is an interaction between the $M_{23}C_6$ (Cr rich carbide) precipitates and dislocations as depicted in Fig. 5.14(b). Dislocation density has decreased in comparison with the specimen tested at RT. The diffraction pattern confirms the presence of gamma matrix and $M_{23}C_6$ precipitate (Fig. 5.14d). The $M_{23}C_6$ precipitates provide grain boundary strengthening to the alloy thereby resulting in increase in strength of the alloy at its service temperature.

Thus, there could be synergistic effect of the strengthening due to DSA and lower modulus at 600°C for modified 9Cr-1Mo steel whereas for Inconel 617 alloy the strengthening is from the precipitates as well as lower modulus of elasticity as compared to room temperature.

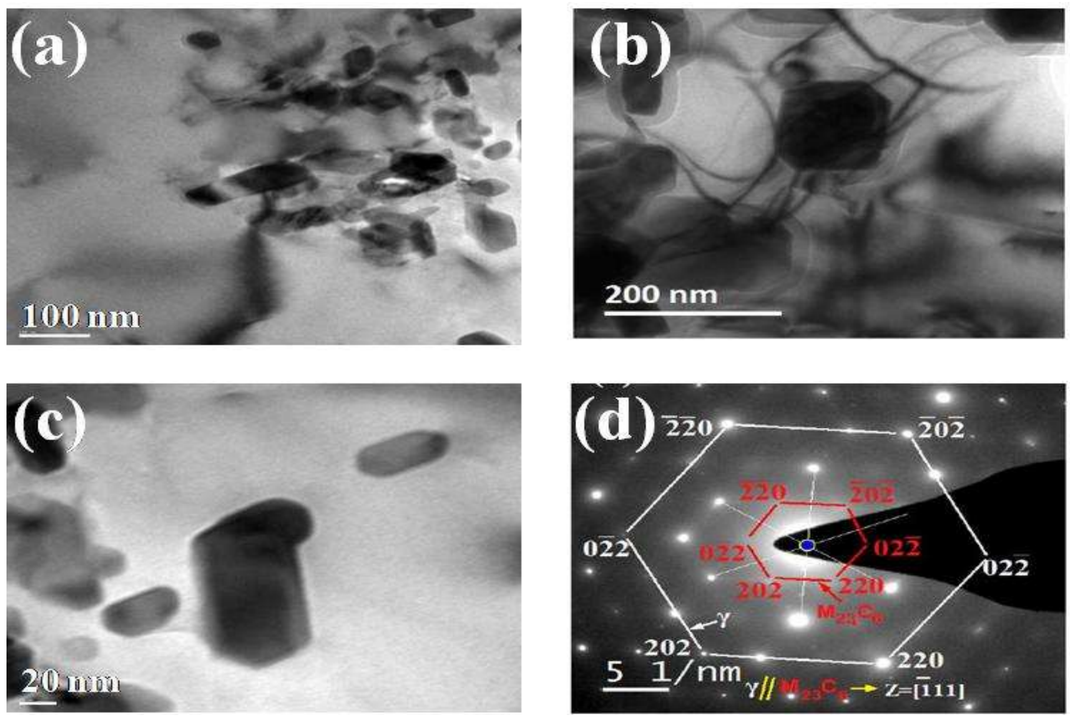

Fig. 5.14 Bright field (BF) TEM micrograph of Inconel 617 alloy, tested at 800^{o}C under asymmetrical loading with mean stress, showing: (a) formation of carbides (b) interaction of dislocations with precipitates (c) magnified view of the second phase particle and (d) SAD pattern confirming gamma matrix and M_{23} C_6 precipitate.

5.5.2 Comparison of ratcheting fatigue behaviour of the alloys at homologous temperature

On comparing the ratcheting strain (Fig. 5.7a, Fig. 5.8a, Fig. 5.9a) and the ratcheting strain rate (Fig. 5.7b, Fig. 5.8b, Fig. 5.9b) plots for both the alloys, it can be very well observed that during initial cycles of stressing, there is abrupt rise in ratcheting strain and rate of accumulation of ratcheting strain in case of Inconel 617 alloy in respect to modified 9Cr-1Mo steel. This can also be observed from Fig. 5.15(a and b) depicting ratcheting strain and ratcheting strain rate plot for Inconel 617 alloy with variation in mean stress from 78 to 165 MPa at constant stress amplitude of 473 MPa at 0.42 T_m. The stepped increase after some cycles of stressing are marked in blocks (Fig. 5.15a). In case of Inconel 617 alloy, the ratcheting strain increased from 20% to 65% depending upon the normalized mean stress and stress amplitude whereas modified 9Cr-1Mo steel showed very stable cyclic behaviour. The fatigue life of modified 9Cr-1Mo steel is higher as compared to that of Inconel 617 alloy. There is stepped increase observed in ratcheting strain for Inconel 617 alloy after certain number of cycles. The 0.42 T_m homologous temperatures of Inconel 617 alloy is also the temperature at which the alloy exhibits dynamic strain aging behaviour.

Dynamic strain aging (DSA) is a process of aging that takes place during plastic deformation over a particular strain rate and temperature range, where the interactions between solute atoms and dislocations, result in a strong pinning of dislocations. A material exhibiting DSA requires higher stresses to produce further straining of the material, either to pull dislocations free from the pinning atoms or to nucleate fresh dislocations. Thus in the ratcheting strain plots, there is observation of steps like increase in the strain that must be due to unpinning effect and due to which there is abrupt increase in the most stabilized region of the ratcheting curve, hence there is reduction in cyclic life of the alloy.

Inconel 617 alloy showed tremendous capability of sustaining such high amount of strain under asymmetrical loading (almost 65%) at normalized mean stress of 0.25 as compared to modified 9Cr-1Mo steel. Therefore, such materials are required to avoid catastrophic failures. Uniform elongation and total elongation are very important parameters for designing of piping and tubing components.

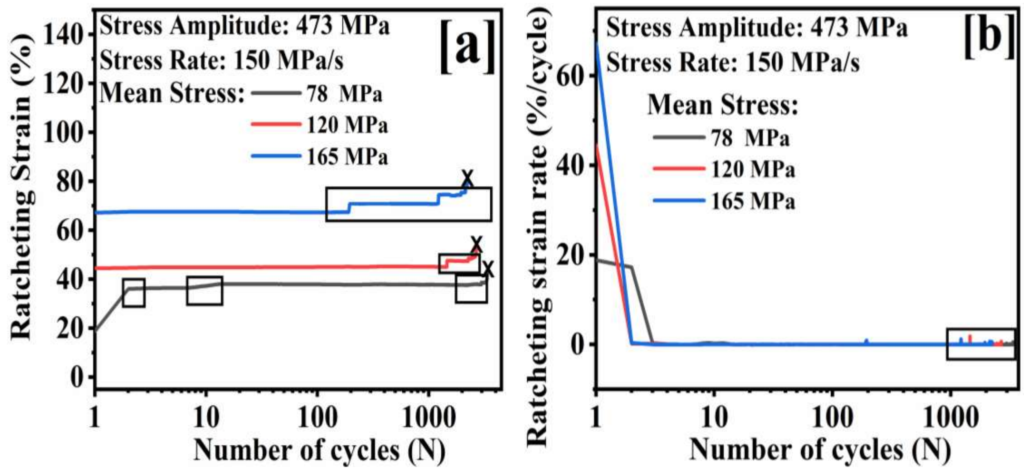

Fig. 5.15 Influence of mean stress on ratcheting at 0.42 T_m for Inconel 617 alloy showing: (a) variation of ratcheting strain with cycles under different mean stress and (b) variation of ratcheting strain rate with cycles.

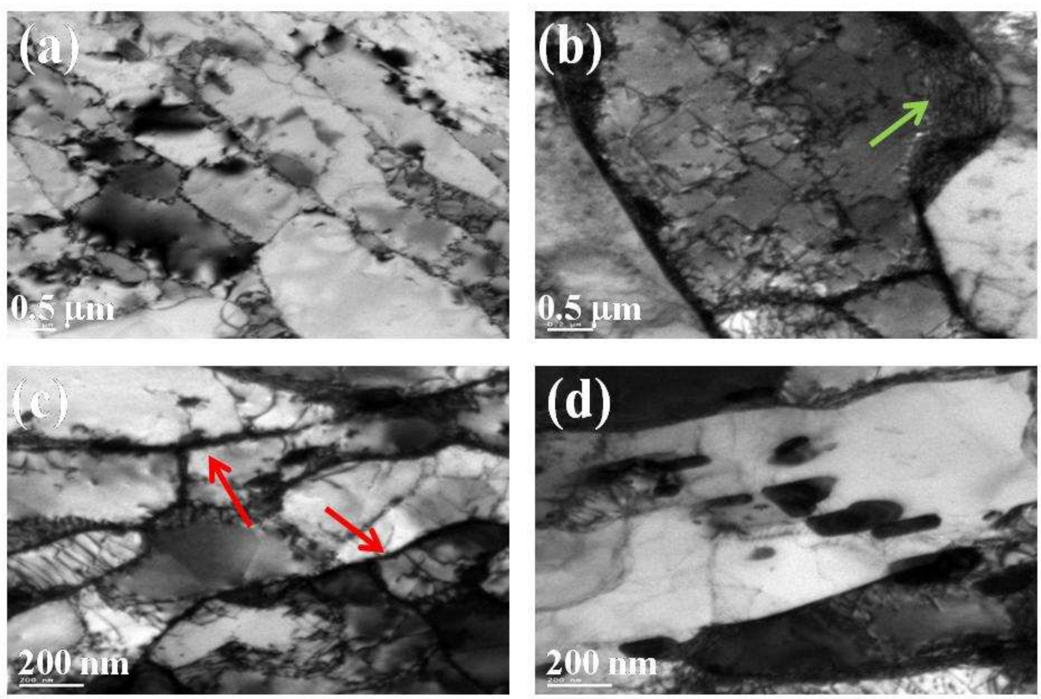

Fig. 5.16 TEM micrographs of modified 9Cr-1Mo steel ratcheted at 0.42 T_m (a) grains clear of dislocations (b) curved boundary (green arrow) (c) dislocations pile-up at boundaries (red arrow) and (d) $M_{23}C_6$ precipitates.

Under asymmetrical stressing the deformation behaviour for modified 9Cr-1Mo steel at 0.42 T_m exhibited clearer grains which are devoid of dislocations (Fig. 5.16a). Due to heavy deformation which consisted of combined effect of temperature and cyclic loading the boundaries are curved (Fig. 5.16b) and also the dislocations are piled up at the boundaries (Fig. 5.16c). The observation of dislocations in Fig. 5.16(a and b) respectively, has been due to difference in the diffraction conditions. The precipitates have also grown in size which means precipitates coarsening (Fig. 5.16d) have also been observed as reported earlier by Verma et al., (2017) under symmetrical strain controlled loading on modified 9Cr-1Mo steel at 600^{o}C.

In case of Inconel 617 alloy slip bands are observed while comparing it with room temperature deformation behaviour it has been observed that more number of slip systems have been activated due to effect of temperature hence, slip bands are observed in more than one direction (intersection of slip bands) as depicted in Fig. 5.17(a), whereas at room temperature slip bands are oriented in one direction hence no intersection of slip bands have been observed. Dislocation tangles have also been observed (Fig. 5.17b).

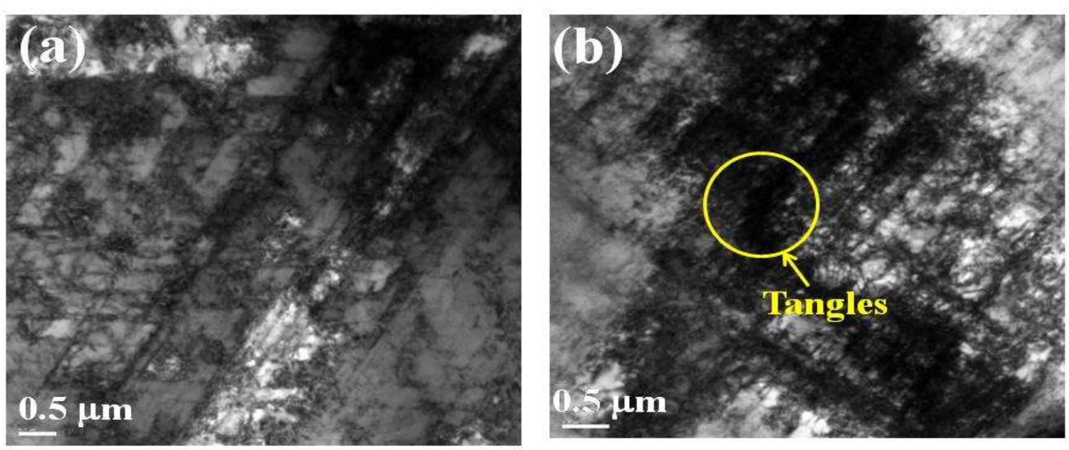

Fig. 5.17 TEM micrographs of Inconel 617 alloy ratcheted at 0.42 T_m (a) intersections of slip bands and (b) tangles of dislocations.

5.6 Summary

The important findings of the ratcheting fatigue behaviour of the alloys at elevated temperatures are summarised below:

1. On comparing the ratcheting behaviour of the alloys at RT with respect to their service temperatures, it was observed that ratcheting strain decreased with increase in temperature thus there was enhancement in fatigue life of the alloy with increase in temperature.
2. The reason behind enhancement in fatigue life with increase in temperature may be attributed to due to the combined effect of DSA and lower modulus of elasticity in case of modified 9Cr-1Mo steel, whereas in case of Inconel 617 alloy, it is due to the formation of precipitates as well as lower modulus of elasticity which imparts strengthening in comparison to RT
3. On comparing the alloys at 0.42 T_m, modified 9Cr-1Mo steel exhibited more significant and stable behaviour with higher fatigue life in comparison with that of Inconel 617 alloy.
4. Inconel 617 alloy showed very high stain accumulation of approximately 65% in comparison to modified 9Cr-1Mo steel and the difference in fatigue life was also of about 600 cycles; thus it can be attributed that under the same parameters though cyclic life is less for Inconel 617 alloy but it can sustain very high strain values.
5. Inconel 617 alloy showed abrupt increase in plastic strain accumulation at 0.42 T_m. The reason behind this may be due to dynamic strain aging of the alloy resulting from unpinning effect. Plastic strain accumulation resulting from pinning of dislocations causes hardening but release of dislocations resulting from unpinning of dislocations causes softening. Strain is localized.

6. Modified 9Cr-1Mo at 0.42 T_m under the same parameters exhibited very stable behaviour and higher cyclic life as compared to Inconel 617alloy. The capability to withstand such high strain values in case of Inconel 617 alloy is very high as compared to modified 9Cr-1Mo steel. Thus it can be concluded that uniform strain plays a very important role at room as well as at elevated temperature for ratcheting fatigue.
7. In ratcheting fatigue, with tensile mean stress, there is progressive increment in the overall length of the specimen; thus, it is obvious that plastic strain in the specimen does not remain localized in the region of slip bands, like that in fatigue under symmetrical loading. Thus, consideration of uniform plastic strain in analysing ratcheting fatigue is quite relevant and important and tensile ductility of material can be considered an important parameter for LCF resistance.
8. The result has been correlated with microstructural features, in case of modified 9Cr-1Mo steel dislocation pile ups and precipitates were observed on the boundaries whereas in case of Inconel 617 alloy intersection of slip bands along with dislocation tangles were observed.
9. At elevated temperatures the fractographic features were similar for both the alloys as observed at room temperature. Modified 9 Cr-1Mo steel exhibited cup and cone type of fracture with striations like features and dimples whereas Inconel 617 alloy showed fatigue type of flat fracture with striations at regular intervals finally leading to overload failure exhibiting dimples.